Optimum Slender Bodies in Hypersonic Flow with a Variable Friction Coefficient

ANGELO MIELE* AND JULIAN COLE†
Boeing Scientific Research Laboratories, Seattle, Wash.

This paper considers the problem of minimizing the total drag of a nonlifting, slender, two-dimensional or axisymmetric body of given length and diameter in hypersonic flow under the assumption that the distribution of pressure coefficients is Newtonian and that the distribution of friction coefficients vs the abscissa is represented by a power law. For the two-dimensional problem, the extremal arc is a wedge regardless of the amount of friction drag and the way it is distributed along the contour. For the axisymmetric problem, the extremal arc includes at most two subarcs, one of which is called the regular shape, and the other, the spike of zero thickness. Furthermore, the solution depends strongly on the friction parameter K_f, which is proportional to the cubic root of the average friction coefficient divided by the thickness ratio. If the friction parameter is less than or equal to a certain critical value K_{fc}, the extremal arc of the axisymmetric problem consists of a regular shape only. For $K_f = 0$, the regular shape is a $\frac{3}{4}$-power body. However, for all other values of $K_f < K_{fc}$, the regular shape is not a power body. If $K_f = K_{fc}$, the regular shape is a power body of exponent $n = 1$ for the constant friction coefficient model, $n = \frac{14}{15}$ for the turbulent flow model, and $n = \frac{5}{6}$ for the laminar flow model. Finally, if $K_f > K_{fc}$, the extremal arc includes a spike of zero thickness and a regular shape. This regular shape is conical only in the constant friction coefficient case; otherwise, it is not conical but approaches a cone in the immediate neighborhood of the axis of symmetry. The difference between the shapes calculated for a constant friction coefficient and those calculated for a variable friction coefficient are of some importance in the laminar flow case but small for the turbulent flow case. For the turbulent regime, it seems entirely permissible to determine the optimum shapes assuming a constant friction coefficient but correcting the drag a posteriori to account for the variation of the friction coefficient along the contour.

1. Introduction

CONSIDERABLE attention has been devoted in recent years to the study of the optimum shapes in hypersonic flow. Although the majority of the papers written on this subject have been concerned with the minimization of the pressure drag, some recent studies[1-4] have been concerned with the minimization of the total drag, that is, the sum of the pressure drag and the friction drag for either slender or thick axisymmetric bodies. In all of these analyses, the friction coefficient was assumed to be constant. Consequently, it is only logical to ask the following question: What is the effect of the variability of the friction coefficient on the geometry of the optimum shapes? The answer is supplied in the subsequent sections under the following assumptions: 1) the body is slender; 2) the distribution of pressure coefficients obeys Newton's impact law; and 3) the distribution of friction coefficients vs the abscissa is represented by a power law.

2. Two-Dimensional Problem

Consider a symmetric airfoil at zero angle of attack in a hypersonic flow, and denote by x a coordinate in the flow direction, y a normal coordinate, and $\dot{y}$ the derivative dy/dx. Observe that, if l is the length, d the thickness, q the free-stream dynamic pressure, C_p the pressure coefficient, and C_f the friction coefficient, the aerodynamic drag per unit span can be written in the form

$$D = 2q \int_0^l (C_p\dot{y} + C_f)\, dx \tag{1}$$

Under the slender-body approximation, the distribution of pressure coefficients is represented by the following simplified form of Newton's impact law[5]:

$$C_p = 2\dot{y}^2 \tag{2}$$

Concerning the distribution of friction coefficients, the power law

$$C_f = A/x^\alpha \tag{3}$$

is assumed with A and α being constant.‡ If C_{fa} denotes the average value of the friction coefficient over the entire length of the body, that is,

$$C_{fa} = \frac{1}{l}\int_0^l C_f dx = \frac{A}{(1-\alpha)l^\alpha} \tag{4}$$

then Eq. (3) can be rewritten in the form

$$C_f = C_{fa}[(1-\alpha)/(x/l)^\alpha] \tag{5}$$

which is used henceforth in this report. After the dimensionless coordinates

$$\xi = x/l \qquad \eta = y/(d/2) \tag{6}$$

are introduced and after the drag coefficient and the thickness ratio are defined as

$$C_D = D/qd \qquad \tau = d/l \tag{7}$$

Received March 4, 1963; revision received July 8, 1963. This paper is a condensed version of the investigation described in Ref. 12. The authors are indebted to Gary R. Saaris for analytical and numerical assistance and helpful discussions.

* Director of Astrodynamics and Flight Mechanics.

† Consultant; also Visiting Professor of Applied Mathematics, Harvard University, Cambridge, Mass.

‡ Typical values of the constant α are 0 for the idealized model in which the friction coefficient is constant, $\frac{1}{5}$ for the turbulent flow model, and $\frac{1}{2}$ for the laminar flow model.

simple manipulations lead to the relationship

$$\frac{C_D}{\tau^2} = \frac{1}{2}\int_0^1 \dot{\eta}^3 d\xi + K_f^3 \qquad (8)$$

where

$$K_f = (2C_{fa})^{1/3}/\tau \qquad (9)$$

is the friction parameter, and $\dot{\eta}$ denotes the derivative $d\eta/d\xi$. From Eq. (8), it is apparent that the friction drag is independent of the geometry of the contour. Consequently, the shape that minimizes the total drag is identical with that which minimizes the pressure drag. The Euler-Lagrange equation characteristic of this shape is given by

$$\ddot{\eta} = 0 \qquad (10)$$

and for the end conditions

$$\xi_i = \eta_i = 0 \qquad \xi_f = \eta_f = 1 \qquad (11)$$

admits the particular solution

$$\eta = \xi \qquad (12)$$

which describes a wedge. The corresponding minimum drag coefficient is given by

$$C_D/\tau^2 = \tfrac{1}{2} + K_f^3 \qquad (13)$$

Incidentally, the conclusion represented by Eq. (12) is valid not only for the assumed power law (3) but also for every other law in which the friction coefficient depends on the abscissa x only.

3. Axisymmetric Problem

Consider a body of revolution at zero angle of attack in a hypersonic flow, and denote by x an axial coordinate, y a radial coordinate, and $\dot{y}$ the derivative dy/dx. Observe that, if l is the length, d the diameter, q the freestream dynamic pressure, C_p the pressure coefficient, and C_f the friction coefficient, the aerodynamic drag can be written in the form

$$D = 2\pi q \int_0^l y(C_p\dot{y} + C_f)dx \qquad (14)$$

Under the slender-body approximation, the distribution of pressure coefficients is represented by Eq. (2). Furthermore, the power law (3) is retained for the distribution of friction coefficients. After the drag coefficient and the thickness ratio are defined as

$$C_D = 4D/\pi q d^2 \qquad \tau = d/l \qquad (15)$$

and after Eqs. (5) and (6) are considered, simple manipulations lead to the fundamental relationship

$$\frac{C_D}{\tau^2} = \int_0^1 \eta\left[\dot{\eta}^3 + 2K_f^3\frac{(1-\alpha)}{\xi^\alpha}\right]d\xi \qquad (16)$$

where K_f is the friction parameter already defined by Eq. (9). After the condition that the slope be nonnegative everywhere is expressed in the form

$$\dot{\eta} - p^2 = 0 \qquad (17)$$

where p is a real variable and after the boundary conditions (11) are specified, the minimal problem is formulated as follows: in the class of functions $\eta(\xi)$ and $p(\xi)$, which are solutions of the differential equation (17) and which are consistent with the end conditions (11), find that special set which minimizes the integral (16).

3.1 The Extremal Arc

In order to solve the proposed problem, a variable Lagrange multiplier $\lambda(\xi)$ is introduced, and the fundamental function is written in the form

$$F = \eta\{\dot{\eta}^3 + 2K_f^3[(1-\alpha)/\xi^\alpha]\} + \lambda(\dot{\eta} - p^2) \qquad (18)$$

so that the Euler-Lagrange equations become[6, 7]

$$\dot{\lambda} + 2\dot{\eta}^3 + 6\eta\dot{\eta}\ddot{\eta} - 2K_f^3[(1-\alpha)/\xi^\alpha] = 0 \qquad (19)$$
$$\lambda p = 0$$

The second of these equations indicates that the extremal arc is generally discontinuous and includes subarcs of the following kinds:

$$p = 0 \qquad \text{or} \qquad \lambda = 0 \qquad (20)$$

Subarcs of the first kind are called zero-slope shapes and are characterized by

$$\dot{\eta} = 0 \qquad \eta = \text{const} \qquad (21)$$

Subarcs of the second kind are called regular shapes and are characterized by $\lambda = 0$ and

$$\dot{\eta}^3 + 3\eta\dot{\eta}\ddot{\eta} - K_f^3[(1-\alpha)/\xi^\alpha] = 0 \qquad (22)$$

Since the extremal arc is generally discontinuous, the Erdmann-Weierstrass corner condition must be applied. After it is observed that the Cartesian coordinates are continuous at a corner point, the conditions in question become

$$\Delta(\lambda + 3\eta\dot{\eta}^2) = \Delta(\lambda\dot{\eta} + 2\eta\dot{\eta}^3) = 0 \qquad (23)$$

where $\Delta(\ldots)$ denotes the difference between quantities evaluated after the corner and before the corner. If the subscript z denotes the zero-slope shape, the subscript r denotes the regular shape, and Eqs. (20) are considered, then the corner conditions can be restated in the form

$$\lambda_z = 3\eta_r\dot{\eta}_r^2 \qquad 0 = \eta_r\dot{\eta}_r^3 \qquad (24)$$

and admit the pair of solutions

$$\begin{aligned} \lambda_z &= 0 \qquad \eta_r = 0 \\ \lambda_z &= 0 \qquad \dot{\eta}_r = 0 \end{aligned} \qquad (25)$$

the second of which is impossible, since it is incompatible with Eq. (22). This leaves only the first solution, so that the following conclusion is reached: a corner point between a zero-slope shape and a regular shape may only occur along $\eta = 0$. Hence, the zero-slope shape is a spike of zero thickness.

Now, if the Legendre-Clebsch condition is employed,[6, 7] it can be shown that the spike must precede the regular shape. Consequently, two alternatives exist: 1) if no corner point is present, the extremal arc consists of a regular shape only; and 2) if a corner point is present, the extremal arc includes a spike of zero thickness followed by a regular shape.

3.2 Power Law Solutions

Since Eq. (22) is nonlinear and has variable coefficients, a general analytical solution may not be obtainable. However, since it is known that many problems of optimum shapes at hypersonic speeds admit power-law solutions, we shall first investigate the existence of particular solutions having the form

$$\eta = \xi^n \qquad (26)$$

Clearly, this equation satisfies the end conditions (11). Furthermore, when substituted into Eq. (22), it leads to the relationship

$$n^2(4n-3)\xi^{3n-3+\alpha} - K_f^3(1-\alpha) = 0 \qquad (27)$$

which can be satisfied identically for every value of the independent variable in only two cases. The first case occurs for

$$K_f = 0 \qquad n = \tfrac{3}{4} \qquad C_D/\tau^2 = \tfrac{27}{64} \qquad (28)$$

Table 1 Critical power law solutions

α	K_{fc}	n_c	$[C_D/\tau^2]_c$
0	1.000	1.000	1.500
$\frac{1}{5}$	0.928	0.933	1.206
$\frac{1}{2}$	0.774	0.833	0.781

and, therefore, yields the $\frac{3}{4}$- power law solution, which is already known from inviscid flow analyses.[5] The second case occurs for

$$K_{fc} = \frac{1}{3}\left[\frac{(3-\alpha)^2(3-4\alpha)}{1-\alpha}\right]^{1/3}$$
$$n_c = \frac{3-\alpha}{3} \tag{29}$$
$$\left[\frac{C_D}{\tau^2}\right]_c = \frac{(3-\alpha)^2(1-\alpha)}{2(3-2\alpha)}$$

This special solution is called the critical solution (Table 1) and is characterized by the following exponents: $n = 1$ if the friction coefficient is ideally constant, $n = \frac{14}{15}$ for the turbulent flow case, and $n = \frac{5}{6}$ for the laminar flow case. The associated values of the friction parameter are especially significant insofar as they determine the existence of two fundamental regimes. As the analysis of Ref. 12 shows, if the friction parameter is subcritical (less than the critical value), the extremal arc consists of a regular shape only. On the other hand, if the friction parameter is supercritical (greater than the critical value), the extremal arc includes a spike of zero thickness and a regular shape.

3.3. Constant Friction Coefficient Solutions

In addition to the inviscid flow case and the critical case already examined in the previous section, the problem of the optimum shape is amenable to a general analytical solution if the friction coefficient is regarded as constant along the contour ($\alpha = 0$). For this case, the differential equation of the regular shape (22) can be rewritten in the form

$$(d/d\xi)[\eta(\dot\eta^3 - K_f^3)] = 0 \tag{30}$$

which admits the general integral

$$\eta(\dot\eta^3 - K_f^3) = K_f^3\gamma \tag{31}$$

where γ is a nonnegative constant.

Positive values of the constant γ correspond to blunt-nosed bodies whose local slope satisfies the inequality $\dot\eta > K_f$ everywhere. Integrating this inequality between the end-points, one deduces that $K_f < 1$. For this subcritical case, the optimum shape is represented by the equation[1]

$$\xi = G(\eta,\gamma)/G(1,\gamma) \tag{32}$$

in which the function G is defined as

$$G(\eta,\gamma) = \int_0^\eta \left(\frac{\eta}{\eta+\gamma}\right)^{1/3} d\eta = [\eta(\eta+\gamma)^2]^{1/3} + \frac{\gamma}{2}\log\frac{(\eta+\gamma)^{1/3} - \eta^{1/3}}{\gamma^{1/3}} - \frac{\gamma}{3^{1/2}}\arctan\frac{3^{1/2}\,\eta^{1/3}}{\eta^{1/3} + 2(\eta+\gamma)^{1/3}} \tag{33}$$

and the constant γ satisfies the condition

$$K_f = G(1,\gamma) \tag{34}$$

The associated drag coefficient is given by[3]

$$C_D/\tau^2 = [\tfrac{3}{2}(1+\gamma)^{2/3} - \gamma K_f]K_f^2 \tag{35}$$

Vanishing values of the constant γ correspond to bodies that are composed of a spike followed by a cone whose slope equals the friction parameter. The integration of the distribution of slopes over the range 0,1 leads to the conclusion that $K_f \geqq 1$. For this supercritical case, the abscissa of the transition point is defined by

$$\xi_0 = 1 - (1/K_f) \tag{36}$$

and the equation of the optimum shape becomes[3]

$$\begin{aligned} 0 \le \xi \le \xi_0 \qquad & \eta = 0 \\ \xi_0 \le \xi \le 1 \qquad & \eta = 1 - K_f(1-\xi) \end{aligned} \tag{37}$$

whereas the associated drag coefficient is

$$C_D/\tau^2 = \tfrac{3}{2}K_f^2 \tag{38}$$

3.4 General Solutions

Except for the analytical solutions corresponding to the cases $K_f = 0$, $K_f = K_{fc}$, and $\alpha = 0$, the integration of the equations governing the optimum shapes must be carried out by means of approximate methods. An important complication occurs because the differential equation of the regular shape (22) exhibits a strong singularity at $\eta = 0$. This singularity can be avoided if the results of the analysis presented in Ref. 12 are employed. Specifically, if the friction parameter is subcritical, the extremal arc includes a regular shape only, and its behavior in the immediate neighborhood of the nose is equal to that of the inviscid flow solution.§ In other words, the body has a blunt nose, and its shape near the axis of symmetry is represented by

$$\eta = C\xi^{3/4} \tag{39}$$

where C is a constant that depends on the friction parameter. On the other hand, if the friction parameter is supercritical, the extremal arc includes a spike of zero thickness and a regular shape. In the immediate neighborhood of the axis of symmetry, the regular shape is no longer blunt-nosed but conical, and its behavior is represented by‖

$$\eta = K_f[(1-\alpha)/\xi_0^{\alpha}]^{1/3}(\xi - \xi_0) \tag{40}$$

where the abscissa of the transition point ξ_0 depends on the friction parameter. Consequently, the practical determination of the optimum shapes is reduced to the following process: 1) if the friction parameter is subcritical, employ Eq. (39) in the interval $0 \le \xi \le \epsilon$, use Eq. (22) in the interval $\epsilon \le \xi \le 1.00$, and match both equations at $\xi = \epsilon$ in such a way that the continuity of the ordinate and the slope is insured; and 2) if the friction parameter is supercritical, employ Eq. (40) in the interval $\xi_0 \le \xi \le \xi_0 + \epsilon$, use Eq. (22) in the interval $\xi_0 + \epsilon \le \xi \le 1.00$, and match the ordinates and the slopes of both equations at $\xi = \xi_0 + \epsilon$. The value of ϵ for which the approximate solutions (39) and (40) are valid depends strongly on the friction parameter, tending to zero as K_f approaches the critical value.

For given values of α and K_f, the integration process requires the guessing of the constant C in the subcritical case and the transition abscissa ξ_0 in the supercritical case. Since the end condition $\eta = 1$ is generally not satisfied at $\xi = 1$, an iteration procedure is necessary in order to determine the relationships

$$\begin{aligned} C &= C(\alpha,K_f) \qquad & K_f \le K_{fc} \\ \xi_0 &= \xi_0(\alpha,K_f) \qquad & K_f \ge K_{fc} \end{aligned} \tag{41}$$

This iteration can be avoided if the auxiliary coordinate

$$\sigma = \eta/K_f \tag{42}$$

is introduced and the problem is transformed from the $\xi\eta$-

§ This is equivalent to stating that the third term of Eq. (22) is negligible with respect to each of the other two.

‖ This is equivalent to stating that the second term of Eq. (22) is negligible with respect to each of the other two.

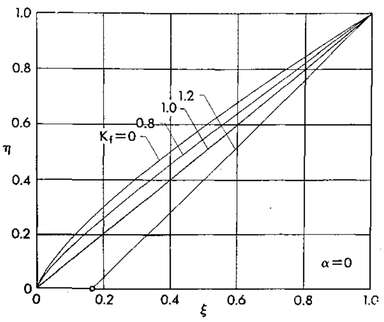

Fig. 1 Extremal solutions for idealized model in which the friction coefficient is constant.

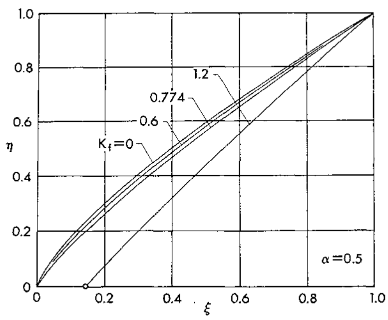

Fig. 3 Extremal solutions for laminar flow model.

plane into the $\xi\sigma$-plane. In this new coordinate system, the equation of the extremal arc becomes

$$\dot{\sigma}^3 + 3\sigma\dot{\sigma}\ddot{\sigma} - [(1-\alpha)/\xi^\alpha] = 0 \text{ (regular shape)}$$
$$\sigma = 0 \text{ (spike)} \tag{43}$$

whereas the end conditions (11) are transformed into

$$\xi_i = \sigma_i = 0 \qquad \xi_f = 1 \qquad \sigma_f = 1/K_f \tag{44}$$

Furthermore, the behavior of the regular shape in the neighborhood of the axis of symmetry is represented by[8]

$$\sigma = C_1\xi^{3/4} \qquad K_f \leq K_{fc}$$
$$\sigma = [(1-\alpha)/\xi_0{}^\alpha]^{1/3}(\xi - \xi_0) \qquad K_f \geq K_{fc} \tag{45}$$

where $C_1 = C/K_f$. For a given value of α, the integration process requires the assigning of arbitrary values to C_1 in the subcritical case and ξ_0 in the supercritical case. Since the end condition $\sigma_f = 1/K_f$ must be satisfied at $\xi = 1$, it becomes possible to determine the relationships

$$K_f = K_f(\alpha, C_1) \qquad K_f \leq K_{fc}$$
$$K_f = K_f(\alpha, \xi_0) \qquad K_f \leq K_{fc} \tag{46}$$

and, thereby, the functions (41) that are relevant to the solution of the problem in the $\xi\eta$-plane.

3.5. Numerical Analyses, Discussion, and Conclusions

With the procedure described in the previous sections, it is possible to determine all the solutions of the proposed problem, whether subcritical, critical, or supercritical. These solutions have the general form

$$\eta = \eta(\xi, \alpha, K_f) \tag{47}$$

whereas the associated drag coefficient is described by the functional relationship

$$C_D/\tau^2 = f(\alpha, K_f) \tag{48}$$

In this connection, numerical analyses have been carried out with an IBM 7090 digital computer, and the results are plotted in Figs. 1–4. The main conclusions are summarized as follows:

1) Power law solutions exist in the inviscid case and the critical case only. For $K_f = 0$, the solution is a $\frac{3}{4}$-power law. For $K_f = K_{fc}$, the solution is a power law of exponent $n = 1$ for the idealized constant friction coefficient model, $n = \frac{14}{15}$ for the turbulent flow model, and $n = \frac{5}{6}$ for the laminar flow model.

2) For $K_f < K_{fc}$, the extremal arc includes a regular shape only. The latter is not a power body but behaves as a $\frac{3}{4}$-power body in the immediate neighborhood of the origin.

3) For $K_f > K_{fc}$, the extremal arc includes a spike of zero thickness and a regular shape. The latter is a cone only if the friction coefficient is constant. If the friction coefficient is not constant, the regular shape is not a cone, even though it approaches a cone in the neighborhood of the axis of symmetry.

4) Regardless of the flow regime, any increase in the friction parameter causes the regular shape to become less convex.

5) The differences between the extremal solutions calculated for a constant friction coefficient and the extremal solutions calculated for a variable friction coefficient are of some importance in the laminar flow case but small in the turbulent flow case.

6) With regard to turbulent flow, it seems entirely permissible to evaluate the optimum shapes assuming a constant friction coefficient. Once the solution is known, one may correct the drag coefficient in order to account for the fact that the friction coefficient varies along the contour.

Since these conclusions are subjected to the approximations (2) and (3) relative to the pressure coefficient and the skin-friction coefficient, a discussion of their validity is in order. Thus, the following statements must be made:

1) For the subcritical solutions, the derivative $\dot{y}$ becomes infinitely large at $x = 0$; hence, the approximations (2) and (3) become locally invalid in the region that immediately surrounds the nose. For the sake of discussion, let this region be defined as the critical region, and let it be identified by the inequality $\dot{y} \gtrsim \tau$. With this hypothesis in mind, it is possible to show that the frontal area associated with the critical region is negligible with respect to the maximum cross-sectional area of the body. For these reasons, the shapes calculated here are close to the shapes that would be predicted with the aid of more accurate laws for the pressure coefficient and the skin-friction coefficient.

2) For the supercritical solutions, the effect of the spike is to reduce the skin-friction coefficient before the body area starts to grow rapidly. In order to exploit this effect, the spike of zero thickness predicted by the theory must be re-

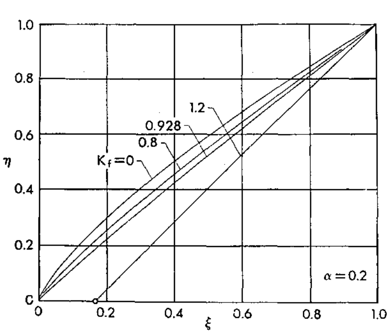

Fig. 2 Extremal solutions for turbulent flow model.

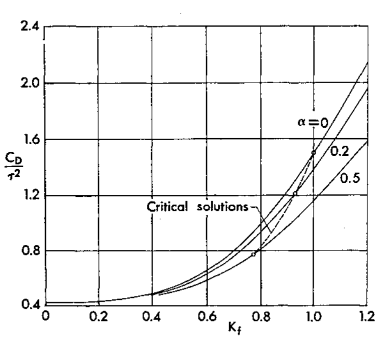

Fig. 4 Minimum drag coefficient vs friction parameter.

placed by a needle having a small but finite thickness. However, this introduces the possibility of flow separation. If the inclination of the body in the neighborhood of the axis of symmetry is sufficiently small and the Reynolds number sufficiently large, the region where the flow separates is presumably small with respect to the over-all body size. Hence, the changes in the distribution of the pressure coefficient and the skin-friction coefficient are small with respect to those assumed here, so that the results of this paper are essentially correct. On the other hand, if the inclination of the body near the axis of symmetry is sufficiently large and the Reynolds number sufficiently small, the extent of the separated region becomes such that the flow pattern assumed in the theory is unrealistic.

References

[1] Kennet, H., "The effect of skin friction on optimum minimum-drag shapes in hypersonic flow," J. Aerospace Sci. **29**, 1486–1487 (1962).

[2] Toomre, A., "Zero-lift minimum drag hypersonic bodies," Grumman Aircraft Engineering Corp., Res. Rept. RE-110 (1959).

[3] Miele, A. and Hull, D. G., "Slender bodies of revolution having minimum total drag at hypersonic speeds," Boeing Scientific Research Labs., Flight Sciences Lab. TR 70 (1963).

[4] Miele, A. and Pritchard, R. E., "Slender two-dimensional bodies having minimum total drag at hypersonic speeds," Boeing Scientific Research Labs., Flight Sciences Lab. TR 71 (1963).

[5] Miele, A., "Optimum slender bodies of revolution in Newtonian flow," Boeing Scientific Research Labs., Flight Sciences Lab. TR 56 (1962).

[6] Miele, A., "The calculus of variations in applied aerodynamics and flight mechanics," Boeing Scientific Research Labs., Flight Sciences Lab. TR 41 (1961).

[7] Miele, A. (ed.), *Extremal Problems in Aerodynamics* (Academic Press, New York, 1964).

[8] Miele, A. and Cole, J., "A study of optimums lender bodies in hypersonic flow with a variable friction coefficient," Boeing Scientific Research Labs., Flight Sciences Lab. TR 66 (1963).

General Bibliography

Chapman, D. R., "Airfoil profiles for minimum pressure drag at supersonic velocities. General analysis with application to linearized supersonic flow," NACA TR 1063 (1952).

Chapman, D. R., "Airfoil profiles for minimum pressure drag at supersonic velocities. Application of shock-expansion theory, including consideration of hypersonic range," NACA TN 2787 (1952).

Eggers, A. J., Resnikoff, M. M., and Dennis, D. H., "Bodies of revolution having minimum drag at high supersonic airspeeds," NACA TR 1306 (1957).

Donaldson, C. D. and Gray, K. E., "Optimization of airfoils for hypersonic flight," Aerospace Eng. **20**, 18–62 (1961).

OCTOBER 1963 AIAA JOURNAL VOL. 1, NO. 10

Electrical Resistance and Sheath Potential Associated with a Cold Electrode

DONALD L. TURCOTTE* AND JAMES GILLESPIE†
Cornell University, Ithaca, N. Y.

The boundary-layer resistance and the difference in sheath potentials between a pair of electrodes have been measured in a shock tube. Using a small, square electrode and a strip electrode flush with the wall of the shock tube, the electric current that could be drawn across the shock tube was measured as a function of the shock wave position for several applied voltages and load resistances. All measurements were made in air at a shock speed of 4.35 mm/μ sec and an initial pressure of 1 mm Hg. In the range of applied voltages considered, the boundary-layer resistance was not a function of the current level. The change in the sheath potential was of the order of several volts. A continuum theory is developed to predict the boundary-layer resistance for small current levels and the sheath potential. The sheath solution is separated from the convective compressible boundary-layer problem where ambipolar diffusion dominates. In the sheath, the transport equations for ions and electrons in an electric field are solved numerically. Resulting integrals for the dimensionless boundary-layer resistance and sheath potential are evaluated, both in the sheath and in the compressible boundary layer, to obtain results that can be compared with experiment. Values of the resistance obtained, assuming the ionization reaction to be frozen, are not in agreement with experiment. Reasonable agreement between theory and experiment is obtained for the magnitude of the sheath potential.

I. Introduction

THE conduction and diffusion of charged particles to a cold electrode are of considerable current interest. One of the important techniques in plasma diagnostics is the use of probes. In order to interpret probe measurements, it is necessary to understand the effect of the cooled region adjacent to the probe. Also, in magnetohydrodynamic devices such as accelerators and generators, an understanding of the electrical losses associated with cold electrodes is of fundamental importance. Sheath studies are also applicable to re-entry problems. At high re-entry velocities considerable ionization occurs. As a result, electrical effects in the boundary layer on the cool re-entry body can have a considerable effect on heat transfer. To obtain a better under-

Presented at the ARS 17th Annual Meeting and Space Flight Exposition, Los Angeles, Calif., November 13–18, 1962; revision received June 3, 1963. This work was supported in part by Therm Advanced Research of Ithaca, N. Y., under a research grant, and in part by the Air Force Office of Scientific Research under Contract AF 49(638)-544. The authors acknowledge the help of Stanley Howard in developing a theory.

* Associate Professor, Graduate School of Aerospace Engineering. Member AIAA.

† Research Assistant, Graduate School of Aerospace Engineering.